Sublimation of Ammonium Salts: A Mechanism Revealed by a First-Principles Study of the NH4Cl System

ARTICLE *in* THE JOURNAL OF PHYSICAL CHEMISTRY C · AUGUST 2007

Impact Factor: 4.77 · DOI: 10.1021/jp073448w

Jeng-Han Wang
National Taiwan Normal University

Sublimation of Ammonium Salts: A Mechanism Revealed by a First-Principles Study of the NH_4Cl System

R. S. Zhu, J. H. Wang, and M. C. Lin*

Department of Chemistry, Emory University, Atlanta, Georgia 30322

Received: May 6, 2007; In Final Form: July 17, 2007

The mechanism for the sublimation of ammonium salts in general is not well-elucidated; the relationship between sublimation energies and activation energies of sublimation has not been understood. We have studied the kinetics and mechanism for the sublimation of NH_4Cl, a prototype ammonium salt, by first-principles calculations using generalized gradient approximation in the plane-wave density functional theory. Supercells containing 8 to 64 NH_4Cl units were used, and the predicted sublimation energy, 41.0 kcal/mol for $NH_4Cl(c) \rightarrow NH_3(g) + HCl(g)$, is in excellent agreement with the experimental value, 42.2 kcal/mol. The result of statistical-theory calculations indicates that the desorption of the $H_3N\cdots HCl$ molecular complex with a 15.5 $\pm$ 1.0 kcal/mol variational barrier, instead of the individual NH_3 and HCl molecules, from the relaxed crystal surface is the rate-controlling step. The desorption rate is predicted to be 25.0 exp($-$13.2 kcal/mol/RT) cm/s, which is in close agreement with the experimental data. This is the first time the sublimation of an ammonium salt has been successfully modeled quantum mechanically. The result supports the heretofore unexplained experimental finding that the activation energy for the sublimation process is significantly lower than the enthalpic change and that the molecular complex of NH_3 and HCl desorbs concurrently as a pair. In addition, the desorption energies of HCl, NH_3, and $H_3N\cdots HCl$ from the neat and relaxed NH_4Cl surfaces have been predicted.

1. Introduction

The mechanism for the sublimation of ammonium salts in general is not well-understood. In this study, we attempt to elucidate the detailed mechanism as well as to predict quantitative kinetics for the sublimation process using NH_4Cl as an example. Ammonium chloride (NH_4Cl) is an important industrial compound. X-ray studies of NH_4Cl at room temperature have shown its structure to be of the CsCl type with a unit cell length of 3.866 Å.[1] Neutron diffraction study indicates that at room temperature the structure involves a disorder in the orientation of ammonium ions, the N−H distance was determined to be 1.03 $\pm$ 0.02 Å.[2] It exhibits interesting sublimation/decomposition phenomena and the mechanism is not clear. Experimentally, Spingler,[3] Schultz and Dekker,[4] and Chaiken et al.[5] have investigated the sublimation kinetics of this system. The mechanism was depicted by Knacke et al.[6] as Scheme 1 where (s) denotes solid, (a) denotes adsorbed species, and (g) denotes gas-phase species. The above mechanism implies that the sublimation of $NH_4Cl(s)$ occurs by the separate and independent desorption of NH_3 and HCl. Experimentally, the activation energy for the sublimation process was reported to be 13.5 $\pm$ 2.0 kcal/mol,[3−5] which is significantly lower than the endothermicity (42.2 kcal/mol)[7] of the process. On the basis of the relatively small 13.5 kcal/mol activation energy, Knacke et al.[6] considered reaction step 1 to be rate-controlling, whereas the results of a hot-plate linear pyrolysis experiment by Schultz and Dekker[4] suggested that desorption step 3 was the rate-determining step. Theoretically, Schultz and Dekker[8] interpreted the decomposition rate on the basis of a modified Langmuir−Hinshelwood bimolecular surface reaction mechanism, giving the desorption rate B $\sim 3.5 \times 10^2$ exp ($-$11.3 kcal/mol/RT) cm/sec. In their calculation, the separate desorption of NH_3 and HCl from the surface was assumed to be the rate-controlling step. The activation energy E_a for the linear vaporization of solid NH_4Cl was assumed to be the sum of heats of adsorption of HCl and NH_3 vapors on their crystal surfaces.[9] It should be pointed out that the crystal surfaces of HCl and NH_3 are characteristically nonionic. No information from a first-principles calculation is available.

SCHEME 1

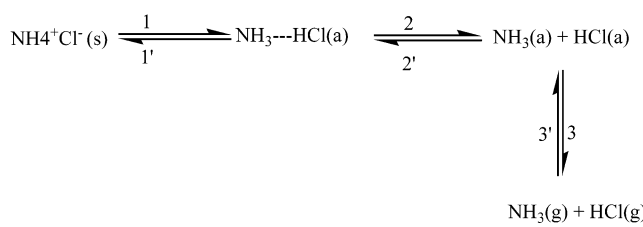

In the present work, the (100) surface of the CsCl structure of NH_4Cl was considered throughout. We have carried out the first quantum-chemical calculation in an attempt to elucidate the mechanism of the sublimation process based on the predicted energetics for the different physical and chemical transformations involved. The predicted results will be compared with existing experimental data.

2. Computational Methods

The calculation was carried out with the Vienna ab initio simulation package (VASP)[10−13] which evaluates the total energy of periodically repeating geometries on the basis of density function theory (DFT) with the pseudopotential approximation. For the periodic boundary condition, the valance electrons were expanded over a plane-wave basis set. The core electron calculations are applied with the cost-effective pseudopotentials implemented in VASP. The expansion includes all plane waves with their kinetic energies smaller than the chosen cutoff energy, that is, $\hbar^2k^2/2m < E_{cut}$, where k is the wave vector,

* Corresponding author. E-mail: chemmcl@emory.edu.

10.1021/jp073448w CCC: $37.00
Published on Web 08/28/2007

TABLE 1: Comparison of the Experimental and Calculated Structural Parameters for NH_4Cl in Crystal Environment Calculated by VASP (Distances in Ångstroms and Angles in Degrees)

parameter	calculated	expt
lattice constant	4.027[a], (4.000)[b], [3.975][c]	3.866[d]
r_{Cl-H}	2.122 ∼ 2.133, (2.134 ∼ 2.142), [2.123]	
r_{Cl-N}	3.124 ∼ 3.135, (3.137 ∼ 3.143), [3.124]	
r_{N-H}	1.025 ∼ 1.050, (1.023 ∼ 1.050), [1.024 ∼ 1.050]	1.03 ± 0.02[e]

[a] 2 × 2 × 2 case (8 NH_4Cl) [b] Values in the parentheses are calculated by 3 × 3 × 3 (27 NH_4Cl) case. [c] Values in the square brackets are calculated by 4 × 4 × 4 (64 NH_4Cl) case. [d] Reference 1. [e] Reference 2.

m is the electronic mass, and E_{cut} is the chosen cutoff energy. In this study, cutoff energies of 400 and 550 eV were chosen for structural parameters and single point energy calculations, respectively.

Generalized gradient approximation (GGA)[14,15] with PW91 exchange-correlation functional[14] was used for the present calculation. The Brillouin-zone (BZ) integration is sampled with $0.05 \times 2\pi$ (1/Å) spacing in reciprocal space by the Monkhorst−Pack scheme.[16] The Fermi-smearing with $\sigma = 0.2$ eV was used. For comparison, different supercells were used in the calculation for elucidation of some characteristics of the system. For the bulk calculation, 8, 27, and 64 NH_4Cl supercells with dimension of $2a \times 2a \times 2a$, $3a \times 3a \times 3a$, and $4a \times 4a \times 4a$ (where a is the lattice constant), along (100), (010), and (001) directions with 3 × 3 × 3, 2 × 2 × 2, and 1 × 1 × 1 Monkhorst−Pack k points, respectively, were employed.

For the calculations of the surface (100), the reconstruction energies, and the decomposition on the surface, the 2 × 2 × 2 model (including 8 NH_4Cl units) was used; the surface is modeled by repeated supercells in three directions: repetition of the in-plane supercells creates an infinite slab, while the periodicity in the direction perpendicular to the slab creates an infinite stack of slabs. To minimize the interaction between the distinct slab surfaces in this infinitely periodic model system, a vacuum region of 36 Å was used to separate the top and bottom surfaces of the slabs; 1 × 5 × 5 Monkhorst−Pack k points (13 irreducible k points) were used in the surface calculation. The dipole corrections were not included in this calculation. On the basis of the optimized crystal structure, the tetrahedron method with Blöchl corrections and the cutoff energy of 550 eV were used to refine the single point energy.

3. Results and Discussion

3.1. Computational Condition Tests. To select a computationally practical and reasonable model, supercells of 2 × 2 × 2 with 8 NH_4Cl units, 3 × 3 × 3 with 27 NH_4Cl units, and 4 × 4 × 4 with 64 NH_4Cl units were employed for the bulk calculations which were performed without any symmetry constraints, and all atomic positions of the molecules were relaxed. The calculated lattice constants are 4.027, 4.000, and 3.975 Å, respectively, from these models as displayed in Table 1. The results show that the lattice constant differences among the 3 models are only about 1%. The values predicted in this work are slightly larger than the experimental value of 3.866 Å.[1] The geometry parameters of NH_4Cl in the crystal environment are also displayed in Table 1. The four N−H bonds in the NH_4 group are not equivalent; the N−H bond pointing to the Cl atom (as shown in Figure 1) is about 0.02 Å longer than the other three. The Cl−H, Cl−N, and N−H bond lengths obtained from the two larger supercells are close to those calculated by the 2 × 2 × 2 model as shown in Table 1. Experimentally, only the N−H bond length, 1.03 ± 0.02 Å, is available.[2] The predicted values in this work are in good agreement with this experimental result.

To further ensure the reliability of the computational results, the structures and frequencies of the isolated gas-phase molecules, NH_3, HCl, and the $H_3N{\cdots}HCl$ complex, which may be the main products on the surface, have been examined by putting isolated HCl, NH_3, and $H_3N{\cdots}HCl$ molecules in a 15 × 15 × 15 Å^3 cubic box with the VASP code and at the B3LYP/6-311+G(3df,2p) level with Gaussian 03.[17] Table 2 displays the calculated and experimental structures of the above molecules. Results of HCl and NH_3 show that the predicted H−Cl and N−H bond lengths agree well with the experimental values,[18] and the differences of these bond lengths calculated by VASP and Gaussian 03 are only 0.005 and 0.004 Å, respectively. Bond angle ∠HNH in NH_3 is calculated to be 0.1° less than that of the experimental value.[18] For the $H_3N{\cdots}HCl$ complex, the differences between VASP and Gaussian 03 are 0.05 and 0.11 Å for H−Cl and N−Cl bond lengths, respectively. If the basis set superposition error (BSSE) corrections[19,20] are included in the B3LYP calculation, the H−Cl bond length is not changed, and the N−Cl bond is only 0.01 Å longer than that obtained without BSSE corrections.

A frequency scaling factor of 0.9614 at the B3LYP/6-311+G-(3df, 2p) level was established[21] and recommended by NIST.[22] The factors at the B3PW91/6-31+G**, B3PW91/6-311G*, and B3PW91/6-311+G(3df,2p) levels[21,22] are 0.9601, 0.9627, and 0.9573, respectively. Therefore, a scaling factor of 0.96 was used for frequency calculations in both methods, as summarized in Table 3. For HCl and NH_3 molecules, except NH_3 symmetric bending mode (ν_6) which has around 7% difference (72 cm^{-1}) obtained by the two methods, the deviations between these methods are less than 3% for the other modes. The corresponding errors between the calculated and the experimental values[23−25] are less than 4%. For $H_3N{\cdots}HCl$, the experimental data[23] shows that the HCl stretching frequency in the complex decreases by more than 1500 cm^{-1}, comparing with that in the isolated HCl molecule.[23] For this and the other vibrational modes of the complex, the experimental values in matrices could not be reproduced by VASP and Gaussian 03 calculations in this work, neither by MP2[26] nor CI[27] calculations. The shifts may be ascribed to the matrix and environment effects.[28] The frequencies for NH_4Cl in the crystal environment were calculated by using the 2 × 2 × 2 model; predicted values are in good agreement with experimental data[29] as shown in Table 3.

3.2. Sublimation Energy. The sublimation energy of the NH_4Cl crystal was calculated as the energy difference between a single fully optimized NH_4Cl molecule in the crystal and that of the gas-phase products, NH_3 + HCl; that is,

$$\Delta H_{sub} = E[NH_3(g) + HCl(g)] - [E(supercell)]/X$$

where, X is the number of NH_4Cl units in the supercell. For the $X = 8$ case, the calculated value, $\Delta H_{sub} = 41.0$ kcal/mol, is close to the experimental value, 42.2 kcal/mol.[7]

The good reproducibility of the experimental values for the sublimation energy, the structures, and the frequencies as discussed above indicates that the 2 × 2 × 2 model is good enough to represent the NH_4Cl crystal.

3.3. Surface and Reconstruction Energies. When a surface is created by cleaving from the bulk material, there will be a rearrangement of atoms near the surface. In order to get an accurate surface energy, one must take into account the surface

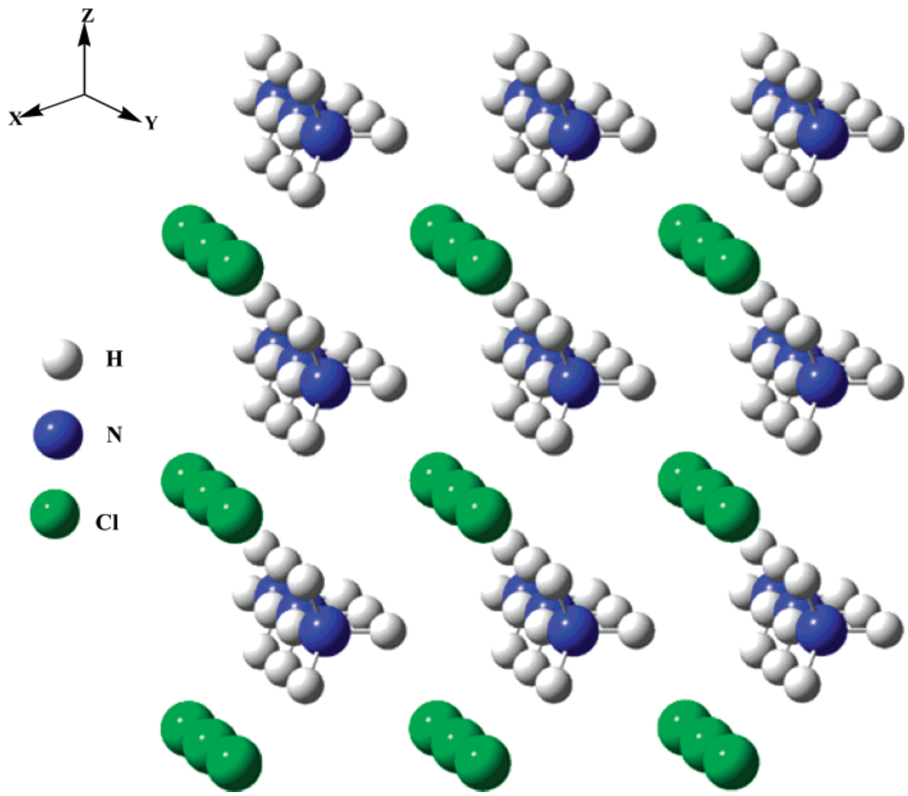

Figure 1. Optimized geometry for the 3 × 3 × 3 NH_4Cl crystal model.

TABLE 2: Structural Parameters for NH_3, HCl, and $H_3N\cdots HCl$ Complex in the Gas Phase Calculated by VASP and at the B3LYP/6-311+G(3df, 2p) Level by Gaussian 03 (Distances in Ångstrom and Angles in Degrees)

parameter	VASP	B3LYP	expt
	HCl		
R_{H-Cl}	1.285	1.280	1.284[a]
	NH_3		
R_{N-H}	1.018	1.014	1.016[a]
∠H−N−H	107.3	107.2	107.3[a]
	$H_3N\cdots HCl$		
R_{H-Cl}	1.389	1.339	
R_{N-Cl}	2.971	3.081	3.136[a]
∠HNH	108.6	108.0	

[a] Reference 18.

relaxation by allowing the surface atoms to reach their minimum energy positions. To prevent the interaction of the desorbed species with the upper surface, the two slabs were separated by 36.0 Å in this work. The surface energy was then calculated according to the following formula:[30]

$$E_{surf}^{relax} = \frac{1}{2S}(E_{slab} - E_{bulk}) \tag{2}$$

where S is the surface area of the slab, E_{slab} is the total energy of the slab with relaxation for all surface atoms, and E_{bulk} is the energy of the bulk containing the same number of NH_4Cl units. The factor of 2 used in eq 2 is because of the two surfaces containing the vacuum space. The predicted value E_{surf}^{relax} in this work is 101.5 mV/Å^2. If E_{slab} is taken as the total energy of the unrelaxed slab, that is, the atomic positions in the slab are fixed, the surface energy for the unrelaxed surface is predicted to be $E_{surf}^{unrelax}$ = 301.2 mV/Å^2. The energy difference of $E_{surf}^{unrelax} - E_{surf}^{relax}$ was defined as the surface relaxation energy.[30] The predicted reconstruction or relaxation energy is 199.7 mV/Å^2, which is 18.7 kcal/mol per NH_4Cl unit. If a bigger 3 × 3 × 3 model was used, the predicted relaxation energy is 17.2 kcal/mol per NH_4Cl unit, which is reasonably close to that obtained with the 2 × 2 × 2 model.

3.4. Desorption Energies of HCl, NH_3, and $H_3N\cdots HCl$ from a Clean NH_4Cl Surface. The desorption energies of $H_3N\cdots HCl$, NH_3, and HCl individually adsorbed on a neat crystal surface of NH_4Cl have been computed. Their adsorption configurations are presented in Figure 2a−c. The desorption energy (E_{des}) was calculated according to the expression

$$E_{des} = E_{molec} + E_{slab} - E_{(molec+slab)}$$

where E_{molec} is the energy of the gas-phase molecule for $H_3N\cdots HCl$, NH_3, or HCl in their equilibrium position, E_{slab} is the total energy of the slab with the 36 Å vacuum space, and $E_{(molec+slab)}$ is the total energy of the adsorbate/slab system. The same conditions have been used to calculate the energies of the bare slab and of the slab−molecule system. For the HCl adsorbed on the surface (see Figure 2a), the molecule is oriented almost perpendicularly to the surface with the Cl atom pointing downward to one of the H atoms in an NH_4 group on the surface with a 2.544 Å Cl···H distance. The predicted E_{des} is 2.6 kcal/mol. For NH_3 adsorption as shown in Figure 2b, the N atom of NH_3 points to one of the H atoms on the surface to form an N···H hydrogen bond with 1.802 Å separation, and the predicted E_{des} is 4.9 kcal/mol. Apparently, the sum of the heats of physical adsorption for HCl and NH_3 vapors on the NH_4Cl crystal surface (2.6 + 4.9 = 7.5 kcal/mol) is less than the activation energy 11.3 kcal/mol estimated by Schultz and Dekker.[8] In the equilibrium configuration of $H_3N\cdots HCl$ adsorbed on the surface as shown in Figure 2c, the Cl atom of the complex connects to one of the H atoms on the surface with a Cl···H hydrogen bond of 2.090 Å; the N−H and the H−Cl bond lengths in the $H_3N\cdots HCl$ pair are 1.216 and 1.583 Å, respectively, which are 0.366 Å shorter and 0.194 Å longer than those in the isolated

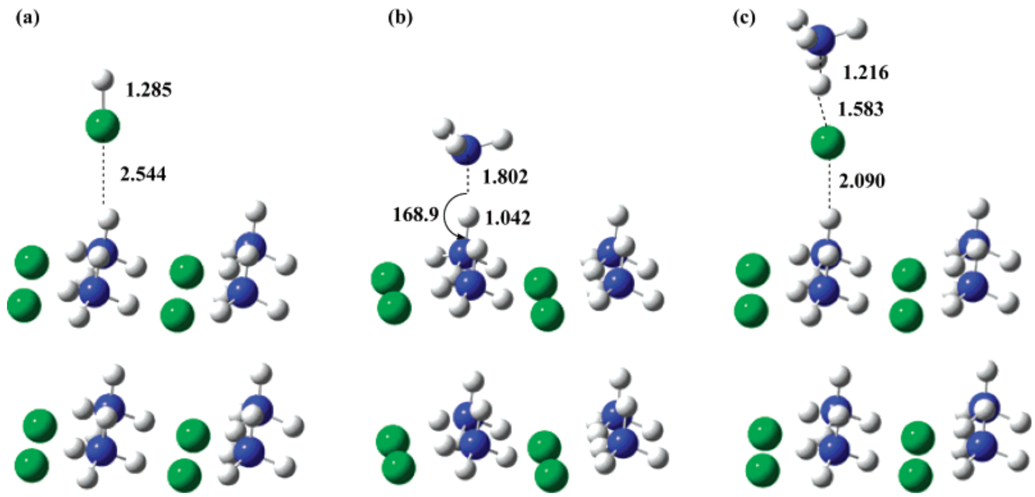

Figure 2. Equilibrium configuration for HCl, NH_3, and HN_3···HCl adsorbed on the pure NH_4Cl surface.

TABLE 3: Comparison of the Experimental and Calculated Vibrational Frequencies Scaled by 0.96[19] by VASP (PW91 in a Plane Wave Basis) and at the B3LYP/6-311+G(3df, 2p) Level for HCl, NH_3, and H_3N···HCl Complex in Gas Phase and NH_4Cl in Crystal

HCl(g)					NH_3(g)				
mode	assignment[a]	VASP	B3LYP	expt	mode	assignment[a]	VASP	B3LYP	expt
ν_1	HCl s	2789	2835	2888[b]	ν_1	NH_3 asym s	3447	3451	3435,[b] 3447[c]
					ν_2	NH_3 asym s	3447	3451	3435,[b] 3447[c]
					ν_3	NH_3 sym s	3311	3339	3337,[d] 3345[c]
					ν_4	NH_3 asym b	1548	1598	1627,[d] 1639[b,c]
					ν_5	NH_3 asym b	1548	1598	1627,[d] 1639[b,c]
					ν_6	NH_3 sym b	916	988	950,[d] 974[b,c]

H_3N···HCl complex (g)					NH_4Cl(s)			
mode	assignment[a]	VASP	B3LYP	expt[b]	mode	assignment	VASP	expt[e]
ν_1	NH_3 asym s	3455	3456	3420	ν_1	NH_4 asym s	3375	3200
ν_2	NH_3 asym s	3454	3455	3420	ν_2	NH_4 asym s	3223	3138
ν_3	NH_3 sym s	3327	3341		ν_3	NH_4 asym s	2928	3044
ν_4	HCl s	1918	2093	1371	ν_4	NH_4 asym s	2865	2810
ν_5	NH_3 asym b	1637	1594		ν_5	NH_4 asym b	1575	1682
ν_6	NH_3 asym b	1636	1593		ν_6	NH_4 asym b	1543	1445
ν_7	NH_3 sym b	1126	1057	1072	ν_7	NH_3 sym b	1404	1403
ν_8	HCl b, NH_3 wag	857	784	1289	ν_8	NH_4 asym b	1354	
ν_9	HCl b, NH_3 wag	856	784	1289	ν_9	NH_4 asym b	1248	
ν_{10}	HCl b, NH_3 rock	279	238	733	ν_{10}	NH_4 rock	293	359 (262)
ν_{11}	HCl b, NH_3 rock	276	237	733	ν_{11}	NH_4 rock	244	
ν_{12}	H_3N−HCl s	203	179	166	ν_{12}	NH_4 rot	176	168

[a] s = stretching, b = bending, wag = wagging, rock = rocking, sym = symmetric, asym = asymmetric, rot = rotation. [b] Reference 23. [c] Reference 24. [d] Reference 25. [e] Reference 29.

gas-phase H_3N···HCl complex, respectively. E_{des} was predicted to be 6.1 kcal/mol. These values, particularly the 7.5 kcal/mol energy sum of HCl and NH_3, are much lower than the experimental sublimation activation energy,[3−5] 13.5 ± 2.0 kcal/mol, indicating that the desorption of HCl and NH_3 from the neat surface cannot represent the sublimation process; in fact, the adsorbed HCl, NH_3, and H_3N···HCl complex may not exist on the neat NH_4Cl surface in view of their low adsorption energies. This result is inconsistent with the mechanism suggested by Schultz and Dekker[8] and depicted by Knacke[6] as shown in Scheme 1.

3.5. Desorption Energies of HCl, NH_3, and H_3N···HCl from a Relaxed Top Layer. The desorption energy E_{des} for HCl, NH_3, and one of the $NH_4^+Cl^-$ molecules desorbing from the relaxed surface is defined as

$$E_{des} = [E_{slab}\,(\text{hole}) + E_{molec}\,(\text{g})] - E_{slab}$$

where E_{slab} (hole) is the energy of the slab after eliminating a molecule (HCl, NH_3, or H_3N···HCl); E_{molec} is the energy of the isolated HCl, NH_3, and H_3N···HCl in the gas phase; and E_{slab} is the total energy of the slab with the 36 Å vacuum space. E_{molec} (g) was calculated in a 15 × 15 × 15 Å^3 cubic box. E_{des} was predicted to be 20.1, 27.0, and 15.5 kcal/mol for HCl, NH_3, and H_3N···HCl desorbing from the top relaxed layer, respectively. These values are much larger than those for the desorption of the same species from a neat NH_4Cl crytalline surface. Significantly, the desorption of HCl and NH_3 individually from the relaxed first surface layer cannot compete with that of H_3N···HCl as a pair. These data indicate that the molecular complex of NH_3 and HCl desorbs concurrently as a pair instead of the separated NH_3 and HCl molecules. To confirm the desorption energy of the H_3N···HCl pair from the relaxed surface, the 3 × 3 × 3 model was also used, and the predicted value, 16.5 kcal/mol at $R = \infty$, is in close agreement with 15.5

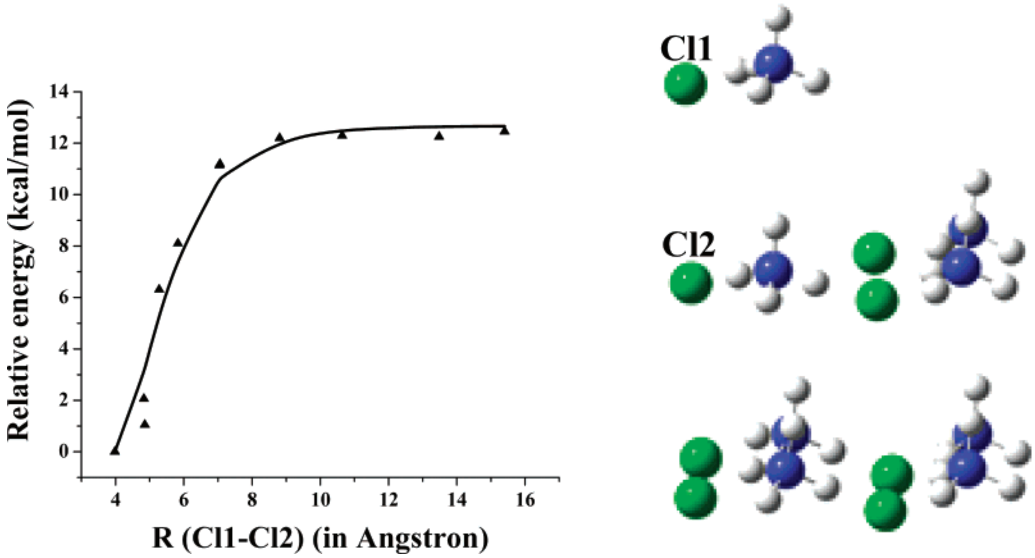

Figure 3. Relative energy for one NH_4Cl molecule dissociated from the relaxed crystal environment, where *R* represents the distance between Cl1 and Cl2 as the configuration indicated in the figure; triangle symbol is the calculated value; solid line is the fitted curve using Morse function.

kcal/mol obtained by the 2 × 2 × 2 model. The desorption−adsorption energy for the NH_3−HCl pair predicted in this work, 15.5 kcal/mol is also in close agreement with 13.5 ± 2.0 kcal/mol of the experimental activation energy for sublimation. Schultz and Dekker[8] and Hill[31] estimated the desorption activation energy of NH_3−HCl to be 10.4 ± (0.6∼2.0) and 11.3 kcal/mol, respectively, by assuming that the activation energy could be approximated by the sum of the heats of physical adsorption of HCl and NH_3 on the NH_4Cl surface. These values are noticeably lower than the 15.5 kcal/mol energy predicted by the 2 × 2 × 2 supercell model calculation.

The desorbed H_3N···HCl(g) complex dissociates rapidly to NH_3(g) and HCl(g) without a distinct transition state as one would expect. The calculated dissociation energy (D_e) for this process by VASP is 11.2 kcal/mol. Experimentally, Goldfinger and Verhaegen[32] reported a D_0 value of 10.0 ± 3.0 kcal/mol, or D_e = 12.3 ± 3.0 kcal/mol if the zero-point energy calculated at the B3LYP/6-311+G(3df, 2p) level was included. With a higher level calculation by CCSD(T)/6-311+G(3df,2p)//B3LYP/6-311+G(3df,2p) using the Gaussian 03 code, D_e for the H_3N···HCl complex is 8.0 kcal/mol. This value should be more reliable.

From the above discussion, we see that one of the $NH_4^+Cl^-$ molecules desorbing from the relaxed surface is the major step of the sublimation process. In order to investigate this process, the 2 × 2 × 2 model was used. The plane consisting of Cl atoms on the first layer was defined as the reference surface, one of the top layer NH_4Cl molecules was pulled off along the *Z* axis from the relaxed surface, the distance between the Cl atom (Cl1) in the dissociated NH_4Cl and another Cl atom (Cl2) in one of the neighboring NH_4Cl lying in the reference surface is defined as *R* as shown in Figure 3. The structure of each point was fully optimized without any constraint. No distinct intrinsic transition state was found in the calculation. The dissociation energy (triangle symbol) with the separation (*R*) is plotted in Figure 3. The selected structures for the relaxed surface and the dissociated product with *R* = 15.4 Å are shown in Figure 4a,b. The result indicates that the proton gradually transfers from NH_4^+ side to Cl^- side as *R* is increasing. In the H_3N···HCl pair at *R* = 15.4 Å (see Figure 4), the N−H and H−Cl bond lengths and Cl−H−N bond angle are 1.375, 1.492 Å and 178.2°, respectively; the other three N−H bonds are 1.025, 1.019, and 1.018 Å. In the gas phase of H_3N···HCl, the corresponding values are 1.582 and 1.389 Å, and 180.0° for N−H and H−Cl bond lengths and Cl−H−N bond angle; the other three N−H bonds are equal with a 1.019 Å value. The relative dissociation energy at *R* = 15.4 Å is 12.4 kcal/mol, which is 3.1 kcal/mol lower than the value (15.5 kcal/mol) at *R* = ∞. To investigate the possible factors producing this difference, the vacuum space of 46 Å and *R* = 15.0 and 20 Å were used; D_e for both cases is 12.3 kcal/mol which is also close to 12.4 kcal/mol under the conditions of 36 Å vacuum space and *R* = 15.4 Å. These values indicate that, with the vacuum space of 36 or 46 Å, the dissociation process already reaches its limit. The dissociation energy deviation may arise from the structural differences of H_3N···HCl calculated in the slab and in its gas phase as shown above. In the slab calculation, 36 or 46 Å vacuum space is added to the *Z* axis, which is enough for the H_3N···HCl gas-phase calculation in this direction. However, in the *X* and *Y* directions, the lattice constant values are kept the same as those in the bulk (8.06 Å); they are not enough for the gas-phase calculation in these two directions. Therefore, the H_3N···HCl pair in the slab at *R* = 15 or 20 Å does not reach the real gas-phase (*R* = ∞ for 3 dimensions) because of the slab limitation, which results in the 3.1 kcal/mol difference as mentioned above. We also tested the dissociation barrier of H_3N···HCl from (010) and (001) surfaces at *R* = ∞; the results show that H_3N···HCl which decomposes from the (001) surface needs a 17.3 kcal/mol barrier, which is 1.9 kcal/mol larger than that from the (100) surface. However, on the (010) surface, we suffered from a convergence problem and did not obtain a definite value.

3.6. Proposed Sublimation/Dissociation Mechanism. On the basis of the above discussion, we suggest that the sublimation/dissociation reaction is a multistage process, which takes place as shown in Scheme 2. In Scheme 2, c refers to $NH_4^+Cl^-$ in the crystal environment (bulk), s refers to the relaxed surface, and g refers to the gas phase. The energy diagram for this process is plotted in Figure 5 in which step 1 involves the surface reconstruction with energy of 18.7 ± 1.0 kcal/mol per NH_4Cl unit as cited above; in step 2, one of the NH_4Cl molecules undergoes proton transfer from NH_4^+ to Cl^- and desorbs from the relaxed surface as a pair, H_3N···HCl(g), with a 15.5 kcal/mol barrier with approximately ±1 kcal/mol energy deviation from the use of different supercell sizes. In step 3, H_3N···HCl(g) dissociates rapidly to NH_3(g) + HCl(g) because of the weak

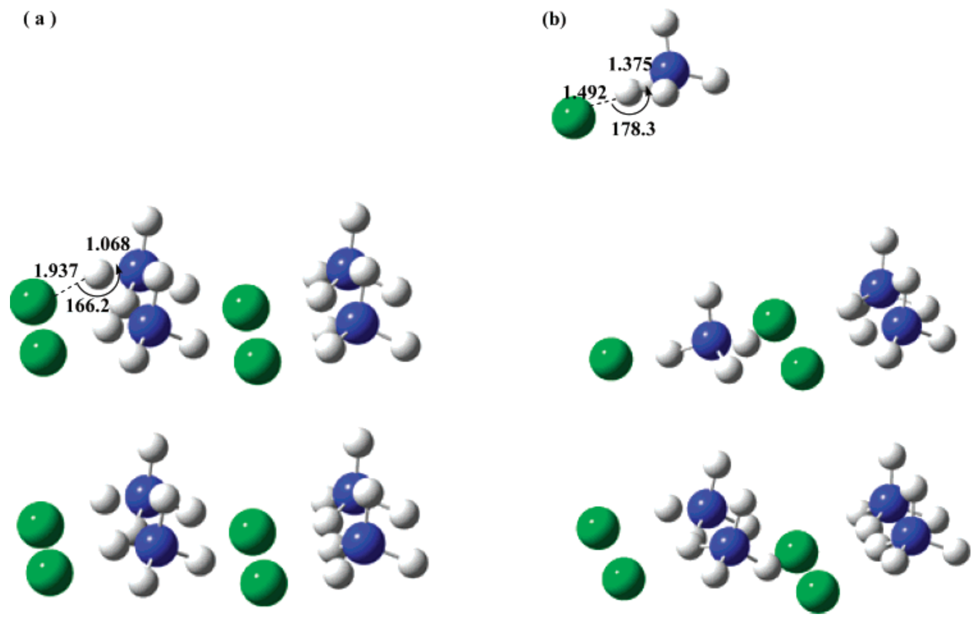

Figure 4. Optimized configurations for (a) the relaxed crystal surface and (b) one of the dissociation products with $R = 15.4$ Å.

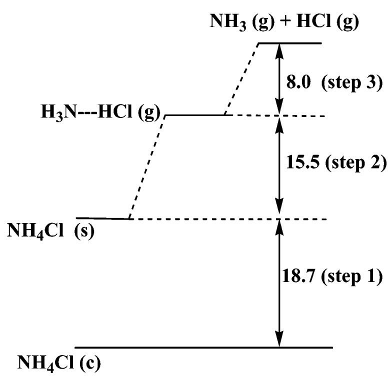

Figure 5. Schematic energy diagram (in kilocalorie per mole) for the sublimation/dissociation processes of NH_4Cl, where NH_4Cl (c) refers to NH_4Cl in the crystal environment; NH_4Cl (s) represents NH_4Cl on the relaxation surface; and $H_3N\cdots HCl(g)$ represents the gas-phase $H_3N\cdots HCl$ pair; [$NH_3(g) + HCl(g)$] represents the products in the gas phase.

SCHEME 2

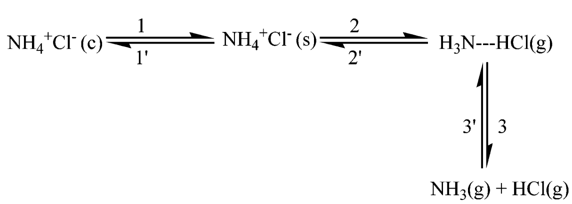

N⋯H bond (1.582 Å) in $H_3N\cdots HCl(g)$ and the low dissociation energy (8 kcal/mol predicted by the CCSD(T) calculation with an uncertainly of about 1−2 kcal/mol). The heat of sublimation estimated from the energies for the 3 steps, 42 kcal/mol with about 10% uncertainty, is in excellent agreement with the 42.2 kcal/mol experimental value as well as with the 41 kcal/mol result predicted for the overall sublimation process, $NH_4Cl(c) \rightarrow NH_3(g) + HCl(g)$ as aforementioned. Apparently, the formation and desorption of the $H_3N\cdots HCl(g)$ pair from the crystal environment (step 2) is the rate-controlling step. The desorption rate for step 2 and the unimolecular dissociation rate for step 3 have been calculated and presented in the following section.

3.7. Prediction of Sublimation Rate. For the sublimation of a solid, the linear rate of regression can be given by the following equation:[4]

$$B = n_s \frac{M}{\rho N} k_s \text{ cm sec}^{-1} \tag{1}$$

in which n_s = number of molecules per cm^2 surface = $(\rho N/M)^{2/3}$; M = molecular weight, g mol^{-1}; ρ = density of solid, g cm^{-3}; N = Avogadro number, molecules mol^{-1}; k_s = molecular desorption rate constant, s^{-1}.

According to the transition state theory,[33]

$$k_s = \frac{k_B T}{h} \frac{Q^*}{Q} \exp(-E_0/k_B T) \tag{2}$$

so that eq 1 becomes

$$B = \left(\frac{M}{\rho N}\right)^{1/3} \frac{k_B T}{h} \frac{Q^*}{Q} \exp(-E_0/k_B T) \text{ cm/s} \tag{3}$$

Here, k_B is the Boltzmann constant, T is the temperature, h is the Planck's constant, E_0 is the energy of activation per molecule at 0 K, and Q^* and Q are the molecular partition function for the transition state and the reactant, respectively.

The decomposition process, $(NH_4Cl)_X \rightarrow (NH_4Cl)_X^* \rightarrow (NH_4Cl)_{X-1} + H_3N\cdots HCl(g)$, is a barrierless dissociation reaction as calculated above for $X = 8$. The potential energy along the minimum energy path (MEP) is shown in Figure 3. The necessary information (the structures, frequencies, etc.) to calculate molecular partition functions for the reactant and transition state is provided by VASP calculations. Transition state parameters for the barrierless decomposition processes were evaluated canonically for each temperature and critical separation, $r^*(T)$, on the basis of the maximum Gibbs free energy criterion as described in refs 34 and 35. The result shows that, in the temperature range of 300−1000 K, the transition state locates at nearly the same configuration. The predicted structures, frequencies, and energies are used in the rate calculations. It should be mentioned that there are several imaginary frequencies corresponding to NH_4^+ rotations in the relaxed surface and the transition state. Fortunately, those imaginary

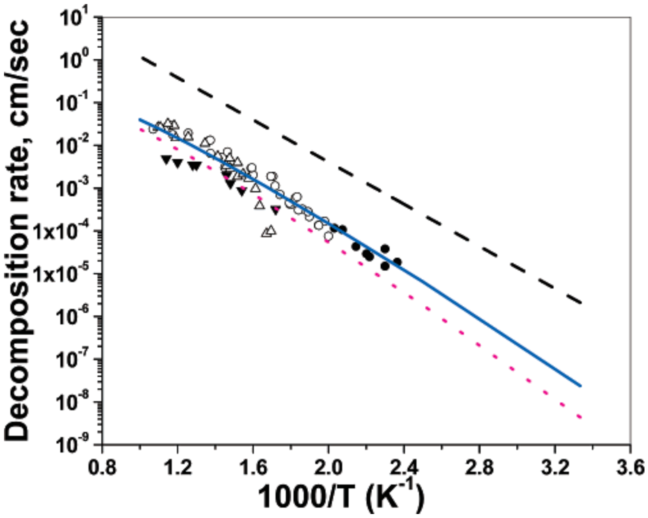

Figure 6. Comparison of the predicted surface regression rates with experimental available values. Symbols are the experimental values: ●, ref 3; ○, ref 5 (at 1−2 mmHg of environmental pressure); △, ref 5 (at 760 mmHg environmental pressure); ▼, ref 4. Dotted and solid lines represent the predicted results in this work using $D_e = 15.5$ and 14.5 kcal/mol, respectively. Dashed line is the estimated value by Schultz and Dekker[8] with the apparent activation energy of 11.3 kcal/mol.

frequencies cancel out from each other in the rate constant calculation. As known, in eq 3, $Q = Q_{trans}Q_{rot}Q_{vib}Q_{ele}$, where Q_{trans}, Q_{rot}, Q_{vib}, and Q_{ele} represent the translation, rotation, vibration, and electronic excitation partition functions, respectively. Among them, only Q_{vib} is related to the molecular frequencies; that is,

$$Q_{vib} = \prod_i (1 - e^{-h\nu_i/kT})^{-1} \tag{4}$$

From eqs 3 and 4, we see that the contribution from the similar imaginary frequencies in the numerator and denominator can be canceled out from each other. Other partition functions given above are taken to be unity.

The temperature (T) resolved method implemented in the Variflex code[36] was used to calculate k_s, and $D_0 = 15.5$ kcal/mol at $R = \infty$ was used in the rate calculation. The predicted values (see Figure 6) are in close agreement with the experimental data of Schultz and Dekker[4] but are slightly lower than those of Spingler[3] and Chaiken et al.[5] The bulk of experimental data can be accounted for with $D_0 = 15 \pm 1$ kcal/mol. The predicted rate constants, $B = 25.0$ exp(−13.2 kcal/mol/RT) and $B = 25.0$ exp(−12.2 kcal/mol/RT) cm/s using $D_0 = 15.5$ and 14.5 kcal/mol, respectively, lie well within the scatter of existing kinetic data. The value estimated by Schultz and Dekker[8] with 11.3 kcal/mol activation energy using the conventional TST was also shown as the dashed line in Figure 6; the result based on their crude and incorrect model overestimates the sublimation rate.

To confirm that the desorption of $NH_4^+Cl^-$ from the relaxed surface is the rate-controlling step, the dissociation rate of $H_3N\cdots HCl(g) \rightarrow HCl(g) + NH_3(g)$ was also calculated using the variational RRKM theory.[37−39] As expected, this process is considerably faster, about 1×10^4 times greater than that of step 2. The rate for this dissociation step can be expressed by 6.92×10^{13} exp(−7.32 kcal/mol/RT) s^{-1}.

4. Conclusion

In this paper, we have performed first-principles calculations using the plane-wave DFT for elucidation of the sublimation/dissociation mechanism of NH_4Cl. The result of our calculations indicates that three distinct steps are involved in the sublimation. In the first step, $NH_4^+Cl^-$ molecules relax from their crystal structure on the surface after cleaving with about 18.7 ± 1.0 kcal/mol relaxation energy (the same energy accounts for the surface structural relaxation after each layer of $NH_4^+Cl^-$ is desorbed in the sublimation process); in the second step, one of the $NH_4^+Cl^-$ molecules on the surface undergoes proton transfer to form an $HN_3\cdots HCl$ complex which desorbs barrierlessly with a 15.5 ± 1.0 kcal/mol energy. In the last step, the molecular complex $HN_3\cdots HCl(g)$ dissociates rapidly also without a distinct barrier to $NH_3(g)$ and HCl(g) with about 8.0 kcal/mol energy. The dissociation rates for steps 2 and 3 were calculated which indicated that step 2 is the rate-controlling step. The predicted overall sublimation endothermicity, sublimation activation energy, and the sublimation rate are in good agreement with available experimental data, quantitatively explaining for the first time that the activation energy for the sublimation of an ammonium salt is significantly lower than the overall enthalpic change and that the molecular complex of NH_3 and HCl desorbs concurrently as a pair.

Acknowledgment. This work was supported by the Office of Naval Research under Grant N00014-02-1-0133. M.C.L. gratefully acknowledges the supports from Taiwan's MOE ATU program as well as the National Science Council and the Taiwan Semiconductor Manufacturing Co. for the NSC-distinguished visiting professorship and the TSMC distinguished professorship, respectively, at the Center for Interdisciplinary Molecular Science, National Chiao Tung University, Hsinchu, Taiwan. We are very much indebted to Taiwan's National Center for High-Performance Computing for the extensive CPUs needed in this work.

References and Notes

(1) Wyckoff, R. W. G. *Crystal Structures;* Interscience Publishers, Inc.: New York, 1951; Vol. I, Chapter III, table p 23.
(2) Levy, H. A.; Peterson, S. W. *Phys. Rev.* **1952**, *86*, 766.
(3) Spingler, H. *Z. Phys. Chem. (Leipzig)* **1942**, *B52*, 90.
(4) Schultz, R. D.; Dekker, A. O. *Fifth International Symposium on Combusion;* Reinhold Publishing Company, Inc.: New York, 1955; p 260.
(5) Chaiken, R. F.; Sibbett, D. J.; Sutherland, J. E.; Van De Mark, D. K.; Wheeler, A. *J. Chem. Phys.* **1962**, *37*, 2311.
(6) Knacke, O.; Stranski, I. N.; Wolff, G. *Z. Phys. Chem. (Leipzig)* **1951**, *198*, 157.
(7) Stephenson, C. C. *J. Chem. Phys.* **1944**, *12*, 318.
(8) Schultz, R. D.; Dekker, A. O. *J. Phys. Chem.* **1956**, *60*, 1095.
(9) Rossini, F. D. U. S. Bureau of Standards Circular 500. *Selected Values of Chemical Thermodynamic Properties*, 1952.
(10) Kresse, G.; Hafner, J. *Phys. Rev. B* **1993**, *47*, 558.
(11) Kresse, G.; Hafner, J. *Phys. Rev. B* **1994**, *49*, 1425.
(12) Kresse, G.; Furthmuller, J. *Comput. Mater. Sci.* **1996**, *6*, 15.
(13) Kresse, G.; Furthmuller, J. *Phys. Rev. B* **1996**, *54*, 11169.
(14) Perdew, J. P.; Yang, Y. *Phys. Rev. B* **1992**, ***45***, 244.
(15) Lee, C.; Yang, W.; Parr, R. G. *Phys. Rev. B* **1988**, *37*, 785.
(16) Monkhorst, H.; Pack, J. *Phys. Rev. B* **1976**, *13*, 5188.
(17) Frisch, M. J.; Trucks, G. W.; Schlegel, H. B.; Scuseria, G. E.; Robb, M. A.; Cheeseman, J. R.; Montgomery, J. A., Jr.; Vreven, T.; Kudin, K. N.; Burant, J. C.; Millam, J. M.; Iyengar, S. S.; Tomasi, J.; Barone, V.; Mennucci, B.; Cossi, M.; Scalmani, G.; Rega, N.; Petersson, G. A.; Nakatsuji, H.; Hada, M.; Ehara, M.; Toyota, K.; Fukuda, R.; Hasegawa, J.; Ishida, M.; Nakajima, T.; Honda, Y.; Kitao, O.; Nakai, H.; Klene, M.; Li, X.; Knox, J. E.; Hratchian, H. P.; Cross, J. B.; Bakken, V.; Adamo, C.; Jaramillo, J.; Gomperts, R.; Stratmann, R. E.; Yazyev, O.; Austin, A. J.; Cammi, R.; Pomelli, C.; Ochterski, J. W.; Ayala, P. Y.; Morokuma, K.; Voth, G. A.; Salvador, P.; Dannenberg, J. J.; Zakrzewski, V. G.; Dapprich, S.; Daniels, A. D.; Strain, M. C.; Farkas, O.; Malick, D. K.; Rabuck, A. D.; Raghavachari, K.; Foresman, J. B.; Ortiz, J. V.; Cui, Q.; Baboul, A. G.; Clifford, S.; Cioslowski, J.; Stefanov, B. B.; Liu, G.; Liashenko, A.; Piskorz, P.; Komaromi, I.; Martin, R. L.; Fox, D. J.; Keith, T.; Al-Laham, M. A.; Peng, C. Y.; Nanayakkara, A.; Challacombe, M.; Gill, P. M. W.; Johnson, B.; Chen, W.; Wong, M. W.; Gonzalez, C.; Pople, J. A. *Gaussian 03*, revision C.01; Gaussian, Inc.: Pittsburgh, PA, 2003.
(18) Woward, N. W.; Legon, A. C. *J. Chem. Phys.* **1988**, *88*, 4694.

(19) Simon, S.; Duran, M.; Dannenberg, J. J. *J. Chem. Phys.* **1996**, *105*, 11024.
(20) Boys, S. F.; Bernardi, F. *Mol. Phys.* **1970**, *19*, 553.
(21) Scott, A. P.; Radom, L. *J. Phys. Chem.* **1996**, *100*, 16502.
(22) Computational Chemistry Comparison and Benchmark Data Base (CCCBDB), release 12, 2005, NIST Standard reference Database 101.
(23) Barnes, A. J.; Beech, T. R.; Mielke, Z. *J. Chem. Soc., Faraday Trans*. 2 **1984**, *80*, 455.
(24) Süzer, S.; Andrews, L. *J. Am. Chem. Soc.* **1987**, *109*, 300.
(25) Shimanouchi, T., Ed. *Tables of Vibrational Frequencies Vol. 1*; National Bureau of Standards Circular No. 39; U.S. GPO: Washington, DC, 1972.
(26) Szczesniak, M. M. ; Kurnig, I. J.; Scheiner, S. *J. Phys. Chem*. **1988**, *89*, 3131.
(27) Bouteiller, Y.; Mijoule, C.; Karpfen, A.; Lischka, H.; Schuster, P. *J. Phys. Chem.* **1987**, *91*, 4464.
(28) Corongiu, G.; Estrin, D.; Murgia, G.; Paglieri, L.; Pisani, L.; Valli, G. S.; Watts, J. D.; Clementi, E. *Int. J. Quant. Chem.* **1996**, *59*, 119.
(29) Wanger, E. L.; Hornig, D. F. *J. Chem. Phys.* **1950**, *18*, 296.
(30) Yang, Z. X.; Woo, T. K. *J. Chem. Phys.* **2004**, *120*, 7741.
(31) Hill, T. L. *J. Chem. Phys.* **1948**, *16*, 181.
(32) Goldfinger, P.; Verhaegen, G. *J. Chem. Phys.* **1969**, *50*, 1467.
(33) Laidler, K. J. *Theories of Chemical Reaction Rates;* McGraw-Hill: London, 1969; Chapter 3.
(34) Hsu, C.-C.; Mebel, A. M.; Lin, M. C. *J. Chem. Phys.* **1996**, *105*, 2346.
(35) Chakraborty, D.; Hsu, C.-C.; Lin, M. C. *J. Chem. Phys.* **1998**, *109*, 8889.
(36) Klippenstein, S. J.; Wagner, A. F.; Dunbar, R. C.; Wardlaw, D. M.; Robertson, S. H. *VARIFLEX: VERSION 1.00*; 1999.
(37) Wardlaw, D. M.; Marcus, R. A. *Chem. Phys. Lett.* **1984**, *110*, 230.
(38) Wardlaw, D. M.; Marcus, R. A. *J. Chem. Phys.* **1986**, *90*, 5383.
(39) Holbrook, K. A.; Pilling, K. J.; Robertson, S. H. *Unimolecular Reactions*; Wiley: Chichester, U.K., 1996.